HEART FAILURE

Accumulation of 5-oxoproline in myocardial dysfunction and the protective effects of OPLAH

Atze van der Pol,[1] Andres Gil,[2] Herman H. W. Silljé,[1] Jasper Tromp,[1,3] Ekaterina S. Ovchinnikova,[1,4] Inge Vreeswijk-Baudoin,[1] Martijn Hoes,[1] Ibrahim J. Domian,[5,6] Bart van de Sluis,[7] Jan M. van Deursen,[8] Adriaan A. Voors,[1] Dirk J. van Veldhuisen,[1] Wiek H. van Gilst,[1] Eugene Berezikov,[4] Pim van der Harst,[1] Rudolf A. de Boer,[1] Rainer Bischoff,[2] Peter van der Meer[1]*

In response to heart failure (HF), the heart reacts by repressing adult genes and expressing fetal genes, thereby returning to a more fetal-like gene profile. To identify genes involved in this process, we carried out transcriptional analysis on murine hearts at different stages of development and on hearts from adult mice with HF. Our screen identified *Oplah*, encoding for 5-oxoprolinase, a member of the γ-glutamyl cycle that functions by scavenging 5-oxoproline. OPLAH depletion occurred as a result of cardiac injury, leading to elevated 5-oxoproline and oxidative stress, whereas OPLAH overexpression improved cardiac function after ischemic injury. In HF patients, we observed elevated plasma 5-oxoproline, which was associated with a worse clinical outcome. Understanding and modulating fetal-like genes in the failing heart may lead to potential diagnostic, prognostic, and therapeutic options in HF.

INTRODUCTION

Heart failure (HF) is one the most challenging health problems of the developed world, with a 5-year survival rate of less than 50% (*1*). Cellular responses to cardiac injury in the failing heart lead to changes in cardiac gene expression and are comparable to patterns observed in the fetal heart (*2*). Most notable is the metabolic switch in energy substrate from fatty acids (postnatal) to carbohydrates (fetal), which is thought to take place by repression of adult and re-expression of fetal genes (*2*, *3*). During HF, several proteins switch back to fetal-like isoforms, including sarcomeric proteins myosin heavy chains and α-actins (*4*). It has been suggested that expression of these fetal-like genes, including several well-known HF-related genes, contributes to the progression of cardiac dysfunction (*2*). Although several aspects of the cardiac fetal-like gene program have been identified, the reoccurrence of the fetal-like gene program in the failing heart remains poorly characterized. The identification of novel genes associated with this process may lead to the identification of novel therapeutic targets in HF.

Here, we set out to further characterize the fetal-like gene program in HF and investigate whether identified genes can affect cardiac function after myocardial infarction (MI). Genes were identified by next-generation RNA-sequencing (RNA-seq) of murine cardiac tissue during development and adult HF. Of the identified genes, we further investigated the role of *Oplah* in murine and human cardiac disease. *Oplah* encodes for 5-oxoprolinase, an enzyme involved in the γ-glutamyl cycle (*5*, *6*), and was shown to be expressed during cardiac development but repressed in HF. OPLAH functions by converting 5-oxoproline, a degradation product of glutathione, to glutamate. The role of the γ-glutamyl cycle in HF has been well established, where dysregulation of several members of this cycle has been associated with the progression and severity of HF, including γ-glutamylcysteine synthetase, glutathione peroxidase, and γ-glutamyltransferase (*7*–*12*). However, the role of OPLAH and 5-oxoproline in cardiovascular diseases has, to date, remained unclear.

[1]Department of Cardiology, University Medical Center Groningen, University of Groningen, 9713 AV Groningen, Netherlands. [2]Department of Pharmacy, Analytical Biochemistry, University of Groningen, 9713 AV Groningen, Netherlands. [3]National Heart Centre Singapore, 169609 Singapore, Singapore. [4]European Research Institute for the Biology of Aging, Laboratory of Stem Cell Regulation and Mechanisms of Regeneration, University of Groningen, 9713 AV Groningen, Netherlands. [5]Cardiovascular Research Center, Department of Medicine, Massachusetts General Hospital, Harvard Medical School, Boston, MA 02114, USA. [6]Harvard Stem Cell Institute, Cambridge, MA 02138, USA. [7]Molecular Genetics Section, Department of Pediatrics, University Medical Center Groningen, University of Groningen, 9713 AV Groningen, Netherlands. [8]Department of Pediatrics, Mayo Clinic, Rochester, MN 55905, USA.
*Corresponding author. Email: p.van.der.meer@umcg.nl

RESULTS

OPLAH is a novel member of the cardiac fetal-like gene program

To identify genes associated with the cardiac fetal-like gene program, we performed RNA-seq on RNA from murine whole-heart embryonic day 12 (E12), left ventricular (LV) tissue at four different stages of cardiac development [E18, postpartum day 2 (PP2), week 4, and week 20 sham], and LV tissue of ischemia/reperfusion (IR)–induced HF (week 20 IR) (Fig. 1A). To specifically target stepwise up-regulated or down-regulated genes, we performed linear regression analysis on the five developmental stages (E12 to week 20 sham). We identified 1266 up-regulated and 1373 down-regulated genes [false discovery rate (FDR), ≤0.05]. The up-regulated genes were highly enriched for genes involved in metabolism and cardiac development, including *Ppar-α*, *Atp2a22* (*Serca2a*), *Atp5b*, and *Pdk2* (table S1), whereas the down-regulated genes were highly enriched for genes involved in cell cycle, including *c-Myc*, *Smad2/3*, and *E2f* (table S2).

To identify genes that were differentially expressed in HF, we compared week 20 sham with week 20 IR. We identified a total of 673 differentially expressed genes (FDR, ≤0.05) in IR-induced HF (203 up-regulated genes and 470 down-regulated genes, including *Myh7*, *Acta1*, *Nppb*, *Ryr2*, and *Fgf2*). Genes involved in the reactivation of the fetal-like gene program were defined as genes that demonstrated inverse expression in HF than during development. Of the 1266 up-regulated genes during development, 39 were down-regulated in HF, and of the 1373 down-regulated genes during development, 29 were up-regulated in HF (Fig. 1, B and C, and table S3). On the basis of KEGG (Kyoto Encyclopedia of Genes and Genomes) pathway analysis, these 68 genes were highly enriched for metabolic and cardiac disease pathways. Of these 68 putative cardiac fetal genes, 39 had already been described in the literature to be associated with cardiac disease or development (including *Ryr2*, *Cacna2d1*, *Fstl1*, and *Bambi*) (*13*–*16*). The remaining 29 genes had been associated with neither cardiac development nor cardiac disease to date and were considered novel genes associated with the cardiac fetal-like gene program.

To evaluate whether these 29 putative cardiac fetal-like genes were also relevant in humans, we screened the expression of these genes across an adult human organ panel using qRT-PCR. *ANXA11*, *HADH*, *CD300LG*, and *OPLAH* were predominantly expressed in the human heart (fig. S1). *CD300LG* was predominantly expressed in adult cardiac tissue, but the expression was barely detectable by qRT-PCR. *ANXA11*, *HADH*, and *OPLAH* were highly expressed in the human adult heart. However, *ANXA11* and *HADH* also had relative high expression in other tissues, compared to *OPLAH*. Therefore, we further explored the role of *OPLAH* in the heart. To test whether *OPLAH* was also induced during human cardiac development, we differentiated human embryonic stem cells (hESCs) to cardiomyocytes. OPLAH protein expression was found to coincide with the expression of the cardiomyocyte marker α-actinin (Fig. 2A). To determine which cellular component of the heart expressed OPLAH, we performed immunoblotting and qRT-PCR on cardiomyocytes, fibroblasts, and endothelial and smooth muscle cells. OPLAH was found to be predominantly expressed by cardiomyocytes (Fig. 2, B to D). Analysis on isolated neonatal rat ventricular cardiomyocytes (NRVCs) revealed that OPLAH was expressed solely in the cytoplasm of cardiomyocytes (fig. S2). To explore the association between cardiac dysfunction and OPLAH expression, we measured OPLAH in three different animal models of HF: IR injury, permanent MI, and pressure overload. In all HF models, OPLAH expression was found to be 50 to 80% lower in failing hearts compared to controls (Fig. 2E, tables S4 to S6, and fig. S3).

Oxidative stress and mechanical stretch deplete OPLAH in vitro

To determine which HF-associated stressors induce OPLAH depletion, we exposed NRVCs to mechanical stretch, isoproterenol (ISO), phenylephrine (PE), and oxidative stress (by administration of hypoxia or H_2O_2). Both ISO and PE are adrenergic stimuli that result in hypertrophy in cardiomyocytes. Neither ISO nor PE administration had an effect on *Oplah* expression (Fig. 2F). With the application of mechanical stretch to NRVCs, we observed a clear reduction in *Oplah* (Fig. 2F and fig. S4), which coincides with an increase in oxidative stress. Similarly,

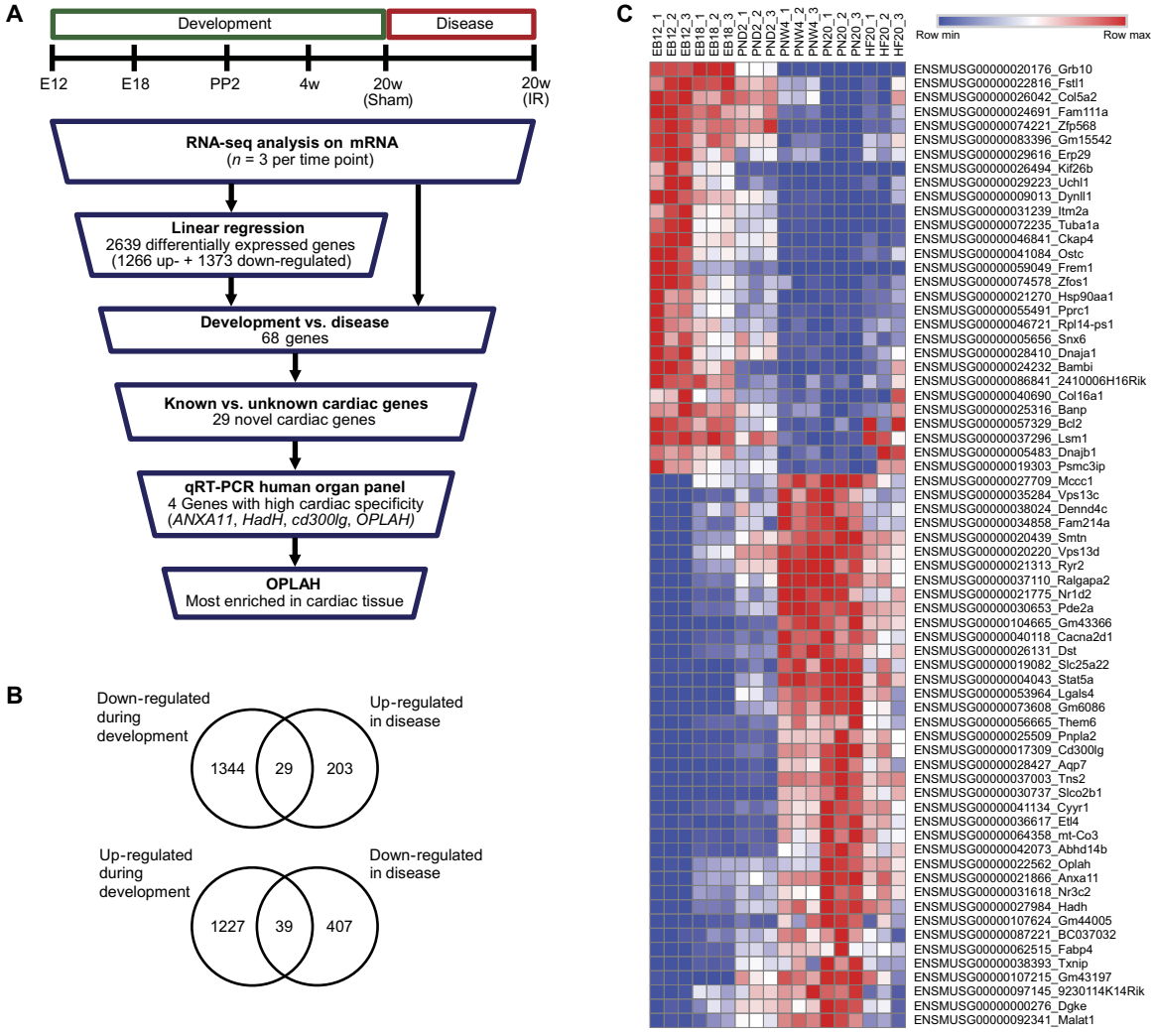

Fig. 1. RNA-seq analysis on the reactivation of the cardiac fetal program. (**A**) Flow chart displaying the steps taken for the identification of novel cardiac fetal genes (*n* indicates the number of murine hearts/left ventricles used). qRT-PCR, quantitative real-time polymerase chain reaction. (**B**) Venn diagram of the number of differentially expressed genes identified in the different groups: up-regulated in development, down-regulated in development, down-regulated in HF, and up-regulated in HF. (**C**) Heat map depicting the expression profiles of the 68 identified cardiac fetal genes during murine development (E12, E18, PP2, 4 weeks old, and 20 weeks old) and cardiac injury (20 weeks old after IR).

hypoxia resulted in a significant reduction in OPLAH expression ($P < 0.0001$; Fig. 2F and fig. S5). Hypoxic culture conditions were maintained for 24 hours, resulting in a significant increase in oxidative stress ($P < 0.001$) and a reduction in medium pH and oxygen concentrations, when compared to controls (fig. S5). To test whether other forms of oxidative stress could also reduce OPLAH expression, we applied H_2O_2 to NRVCs. Exposure to a concentration of 500 μM of H_2O_2 for 12 hours was sufficient to induce a significant reduction in OPLAH ($P < 0.0001$) coupled to a significant increase in oxidative stress ($P < 0.01$; Fig. 2E and fig. S6). Stretch, hypoxia, and H_2O_2 are stressors that can induce myocyte death; to exclude myocyte death as the cause of *Oplah* reduction, we measured trypan blue–positive cells and lactate dehydrogenase release and performed qRT-PCR for BCL2 and BAX expression (figs. S4, B to D, S5, C to E, and S6, A to C). In all cases, we found an increase in cardiomyocyte death. However, the percentage of cell death could only partially explain the reduction in *Oplah* expression observed. Finally, because we found OPLAH to be markedly depleted with the induction of oxidative stress, we investigated whether mechanical stretch, which depleted OPLAH, also resulted in an increase in oxidative stress. We found a 25% increase in oxidative stress in stretched cardiomyocytes compared to controls (fig. S4A). These findings indicate that OPLAH depletion is influenced by stretch and oxidative stress. The latter is of particular interest because OPLAH is associated with the formation of the antioxidant glutathione.

OPLAH expression is associated with oxidative stress in vitro

To identify whether OPLAH had an in vitro effect on oxidative stress in cardiomyocytes, we developed adenovirus harboring short hairpin RNA (shRNA) knockdown vectors of *Oplah* (shOPLAH) and cardiac-specific human *OPLAH* overexpression vectors (hOPLAH) (Fig. 2G and fig. S7). To test whether our shOPLAH and hOPLAH constructs were functional in vitro, we developed a liquid chromatography–mass spectrometry (LC-MS) method to measure 5-oxoproline, the substrate for OPLAH. In cell lysates of NRVCs infected with shOPLAH, we found

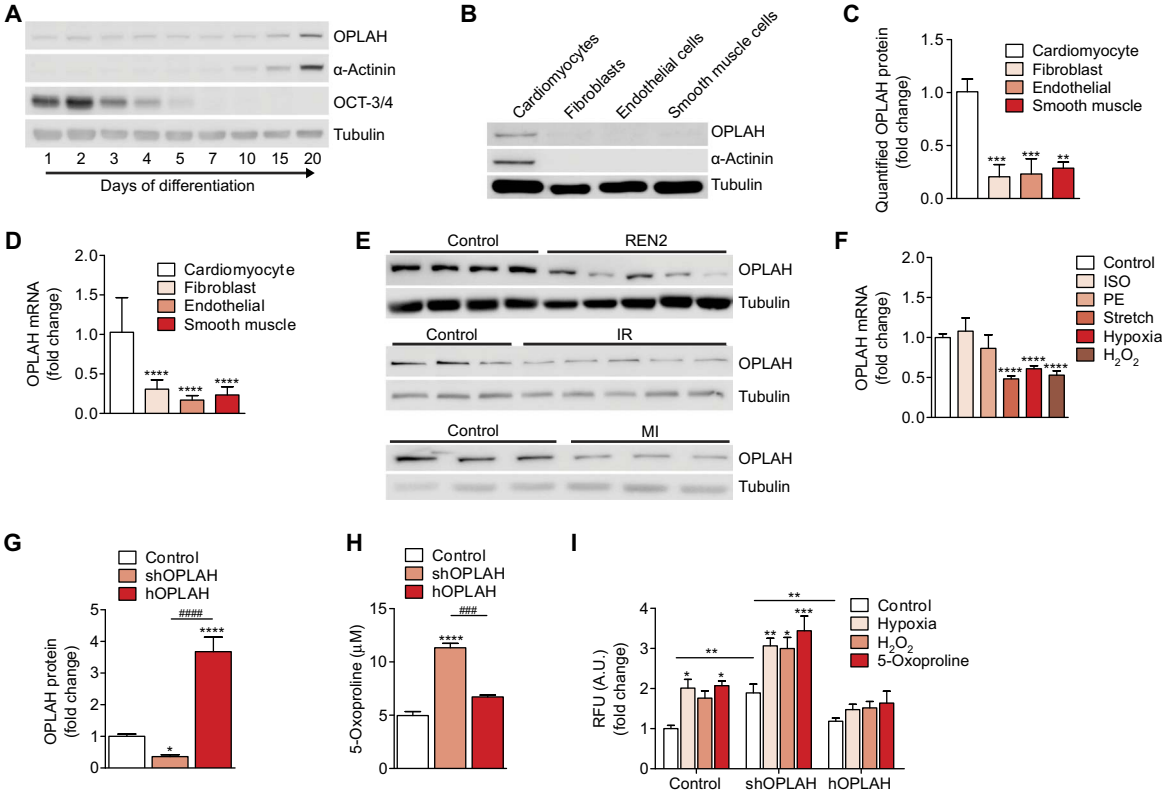

Fig. 2. OPLAH in vitro characterization. (**A**) Representative immunoblotting analysis of OPLAH expression during hESC cardiomyocyte differentiation. (**B**) Representative immunoblotting analysis of OPLAH protein expression in NRVCs, rat fibroblasts, murine endothelioma cells, and rat smooth muscle cells. (**C**) Quantified OPLAH protein expression in NRVCs ($n = 4$), rat fibroblasts ($n = 4$), murine endothelioma cells ($n = 4$), and rat smooth muscle cells ($n = 5$). (**D**) qRT-PCR mRNA expression of OPLAH in NRVCs ($n = 7$), rat fibroblasts ($n = 8$), murine endothelioma cells ($n = 8$), and rat smooth muscle cells ($n = 8$). (**E**) Immunoblotting analysis of OPLAH expression in three animal models for HF. Top: OPLAH expression in Sprague Dawley rats (control; $n = 4$) versus renin overexpression TG rats (REN2; $n = 5$). Middle: OPLAH expression in sham (control; $n = 3$) versus IR ($n = 5$) C57BL/6 mice. Bottom: OPLAH expression in sham (control; $n = 3$) versus MI ($n = 3$) rats. (**F**) qRT-PCR mRNA expression of OPLAH in NRVM exposed to ISO ($n = 4$), PE ($n = 4$), stretch ($n = 17$), hypoxia ($n = 31$), H_2O_2 ($n = 16$), and no-treatment controls ($n = 23$). (**G**) Quantified OPLAH protein expression in NRVCs infected with the control, short hairpin OPLAH (shOPLAH), or human OPLAH overexpression (hOPLAH) constructs ($n = 6$, 11, and 5, respectively). (**H**) 5-Oxoproline concentrations in NRVCs infected with the control, shOPLAH, or hOPLAH adenoviral construct ($n = 3$). (**I**) CellROX analysis of adenoviral-infected NRVCs with control, shOPLAH, or hOPLAH vector exposed to 24 hours of hypoxia, 24 hours of H_2O_2 (500 μM), or 2 hours of 5-oxoproline (10 mM) culture conditions [for all conditions, $n = 10$ (control), 15 (shOPLAH), and 15 (hOPLAH)]. CellROX data are presented as fold change of relative fluorescence units (RFU) [arbitrary units (A.U.)] per microgram protein. Data are presented as means ± SEM. $^{*}P < 0.05$; $^{**}P < 0.01$; $^{***}P < 0.001$; $^{****}P < 0.0001$; $^{\#\#\#}P < 0.001$; $^{\#\#\#\#}P < 0.0001$, as calculated by Student's *t* test or one-way analysis of variance (ANOVA). "*" indicates significant difference compared to control, whereas "#" denotes differences between groups other than control. *n* indicates the number of biological replicates of cell experiments or the number of animals.

a significant increase in intracellular 5-oxoproline ($P < 0.0001$; Fig. 2H). This increase in 5-oxoproline was coupled to an increase in reactive oxygen species (ROS) (Fig. 2I). The increase in ROS was more pronounced under hypoxic or H_2O_2 culturing conditions (Fig. 2I). NRVCs infected with hOPLAH were protected, to a large extent, from hypoxia and H_2O_2-induced oxidative stress (Fig. 2I). Previous publications have demonstrated that 5-oxoproline can itself induce oxidative stress in neurons (*17*, *18*). This finding is supported by our data, where a decrease in OPLAH leads to increased 5-oxoproline and oxidative stress. To further demonstrate that 5-oxoproline is an oxidative stress–inducing agent, we exposed NRVCs to exogenous 5-oxoproline. The administration of 5-oxoproline resulted in an increase in ROS production in cardiomyocytes under control culture conditions, which was amplified when OPLAH was depleted, but diminished when OPLAH was overexpressed (Fig. 2I).

ERRα, and not ERRγ, transcriptionally regulates OPLAH expression in vitro

To understand the regulation of *Oplah*, we were interested in identifying transcription factors involved in the expression of OPLAH. A recent study has shown by means of ChIP (chromatin immunoprecipitation)–on–chip analysis that the estrogen-related receptor α (ERRα) and ERRγ both have high affinity for the *Oplah* promoter (*19*). However, direct regulation of *Oplah* by these transcription factors has not been demonstrated. To study the effects of ERRα and ERRγ on OPLAH expression, we exposed NRVCs to XCT-790 [ERRα antagonist (*20*)] and 4-hydroxytamoxifen [ERRγ antagonist (*21*)]. 4-Hydroxytamoxifen demonstrated no effect on *Oplah* expression, whereas exposure to XCT-790 resulted in a dose-dependent reduction in *Oplah* coupled to an increase in ROS (fig. S8). To test whether this mechanism was also present in human cardiomyocytes, we exposed cardiomyocytes derived from hESCs to XCT-790 and 4-hydroxytamoxifen and observed similar results (Fig. 3, A to C). Inhibition of ERRα in the human cardiomyocytes led to an increase in transcription of *ERRα* and *PGC-1α* [a coactivator and transcriptional regulator of ERRα (*22*, *23*)], suggesting a compensatory mechanism for the lack of functional ERRα (Fig. 3, D to E). To determine whether the increase in ROS by the ERRα antagonist was a consequence of a reduction in *OPLAH*, we administered hOPLAH adenovirus to cardiomyoblasts before treatment with XCT-790. OPLAH overexpression reduced the XCT-790–induced oxidative stress (Fig. 3F). qRT-PCR analysis on cardiac tissue from different stages of development and disease showed that the *Errα* expression profile resembled that of *Oplah* (Fig. 3G). Under in vitro conditions known to induce OPLAH repression (stretch, hypoxia, and H_2O_2), we found that *Errα* expression was reduced, coinciding with *Oplah* depletion (fig. S9). Overall, these findings suggest that ERRα, and not ERRγ, is involved in the transcriptional regulation of OPLAH in cardiomyocytes.

Cardiac-specific OPLAH overexpression protects mice from IR injury

To test whether the protective effects of OPLAH in cultured cardiomyoblasts and NRVCs translate into a therapeutic effect, we created OPLAH-transgenic (OPLAH-TG) mice with cardiomyocyte-specific hOPLAH overexpression (Fig. 4A). Immunoblotting and qRT-PCR revealed that OPLAH mRNA and protein expression was elevated in the hearts of male OPLAH-TG mice compared to wild-type (WT) littermates (Fig. 4, B to D). In other tissues, including the kidneys, no difference in OPLAH expression was observed between WT and OPLAH-TG mice, confirming that overexpression was confined to the heart. At baseline, the OPLAH-TG mice had comparable body weight, organ weight (right ventricle, left ventricle, atria, kidney, and liver), heart rate, LV ejection fraction, stroke volume, and systolic and diastolic blood pressure to their WT littermates.

To test whether OPLAH-TG mice were protected against oxidative stress–induced cardiac damage, we exposed mice to 60 min of ligation of the anterior descending branch (LAD) of the left coronary artery (ischemia), followed by 4 weeks of reperfusion. OPLAH-TG mice had significantly smaller infarct sizes compared to WT littermates after IR injury, as measured by Masson's trichrome staining ($P < 0.05$; Fig. 4E). There was a significant increase in LV weight after IR in the WT mice, an effect that was not present in the TG mice ($P < 0.0001$; table S7). The TG mice had reduction in the mRNA expression of fibrotic markers TIMP-1 and Col1a1 when compared to the WT mice after IR (fig. S10). Cardiac magnetic resonance imaging (MRI) and Millar hemodynamics measurements revealed that the TG mice had a higher LV ejection fraction and larger stroke volume after IR when compared to the WT mice (Fig. 4F). Cell size increased after IR; however, no significant differences between WT and TG mice were observed ($P = 0.2934$; fig. S11). Cleaved Caspase-3 staining on the left ventricle demonstrated that there was an increase in the number of apoptotic cells; however, the difference between groups was not significant ($P = 0.3784$; fig. S12). In WT mice, we observed a reduction in ERRα and OPLAH expression after IR (Fig. 4G), and the decrease in OPLAH in the WT mice resulted in substantially higher 5-oxoproline in cardiac tissue when compared to the OPLAH-TG mice (Fig. 4H). To test whether the observed reduction in 5-oxoproline in the OPLAH-TG mice after IR lowered oxidative stress, we measured the total antioxidant capacity (TAC) and the ratio of reduced glutathione (GSH) to oxidized glutathione (GSSG) in LV tissue. We found a significant decrease in TAC ($P < 0.05$) and GSH/GSSG ratio ($P < 0.05$) in the WT mice after IR injury that was not observed in OPLAH-TG mice (Fig. 4, I and J). These data suggest that when murine hearts are exposed to oxidative stress in the form of IR injury in vivo, cardiomyocyte-specific overexpression of OPLAH reduces 5-oxoproline–induced oxidative stress, resulting in reduced infarct size and ultimately leading to improved cardiac function.

Cardiac-specific OPLAH overexpression protects mice from permanent MI

To study the effects of OPLAH overexpression in a more severe form of cardiac injury, we exposed WT and OPLAH-TG mice to permanent MI (table S8) by ligating the LAD of the left coronary artery. Similar to IR injury, OPLAH-TG mice demonstrated a significant improvement in stroke volume 4 weeks after ligation compared to WT mice ($P < 0.01$; Fig. 5A). OPLAH-TG mice had significantly smaller infarct sizes ($P < 0.05$; Fig. 5B) and a reduction in cleaved Caspase-3–positive cells, compared to WT mice after MI (fig. S12). Furthermore, we also observed a decrease in 5-oxoproline in the OPLAH-TG mice coupled to an improved GSH/GSSG ratio, suggesting a decrease in oxidative stress (Fig. 5, C to E).

Circulating 5-oxoproline is elevated in patients with HF and predicts outcome

Because LV tissue 5-oxoproline concentrations were increased in HF animals compared to sham controls, we explored whether this increase could also be found in the plasma of these animals, in hopes of identifying a potential circulating biomarker. In rats with pressure overload–induced HF (REN2) where LV tissue 5-oxoproline was ~20-fold higher than in control rats, circulating 5-oxoproline was also found to be about sixfold higher (Fig. 6, A and B). To determine whether these findings could be extrapolated to the human setting,

we measured 5-oxoproline in the plasma of healthy controls (n = 10) and patients with acute HF (n = 10) (*24*). Plasma 5-oxoproline was increased about fourfold in acute HF patients compared to healthy controls (Fig. 6C).

To further elucidate the potential of 5-oxoproline as a circulating biomarker in clinical HF, we tested the prognostic potential of 5-oxoproline in a cohort of 535 patients who had been hospitalized for acute HF (table S9) (*25*). The patients were monitored for 18 months, and the combined primary end point of the study was all-cause mortality and HF hospitalization (*26*–*28*). Patients with higher 5-oxoproline had a higher incidence of atrial fibrillation and higher N-terminal pro–brain natriuretic peptide (NT-proBNP) and glutamate (tables S9 and S10). 5-Oxoproline was associated with known biomarkers for cardiac remodeling, stretch, and oxidative stress, but not with inflammation (table S11). When looking at the primary end point, we found that higher 5-oxoproline was associated with a worse outcome (Fig. 6D). In multivariable analyses corrected for age, sex, renal function, history of atrial fibrillation, and NT-proBNP concentration, the highest tertile of 5-oxoproline remained significantly associated with a higher risk of reaching the primary combined end point compared to risk nadir [hazard ratio (HR), 1.54; 95% confidence interval (CI), 1.09 to 2.17; P = 0.013; tables S12 and S13] as well as to the lowest two tertiles (HR, 1.42; 95% CI, 1.09 to 1.85; P = 0.009). These data suggest that circulating 5-oxoproline, the substrate of OPLAH, has diagnostic and prognostic potential in patients with HF.

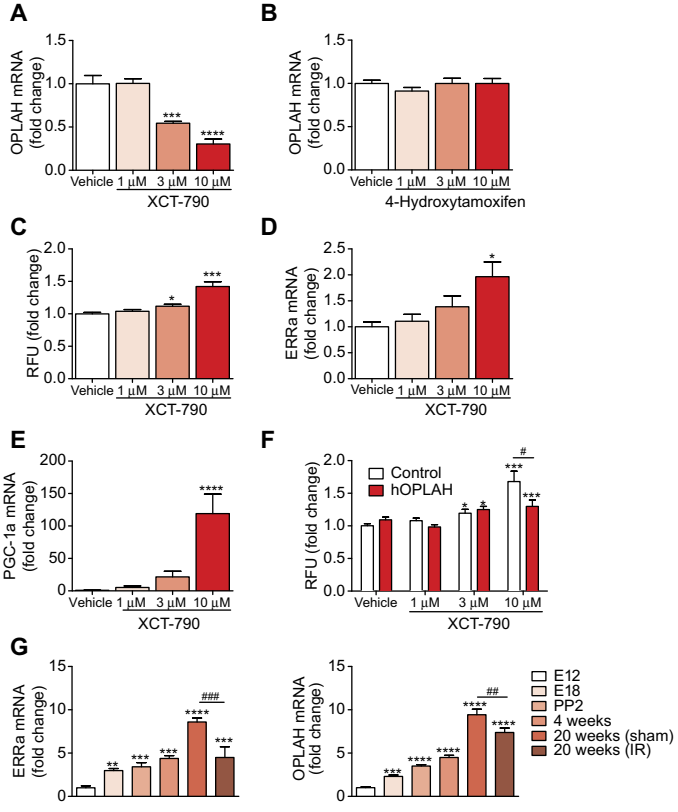

Fig. 3. ERRα is involved in the regulation of OPLAH. (**A**) OPLAH expression in hESC-derived cardiomyocytes exposed to increasing concentrations of XCT-790 (vehicle, n = 6; 1 μM, n = 6; 3 μM, n = 6; 10 μM, n = 4). (**B**) OPLAH expression in hESC-derived cardiomyocytes exposed to increasing concentration of 4-hydroxytamoxifen (vehicle, n = 5; 1 μM, n = 6; 3 μM, n = 6; 10 μM, n = 5). (**C**) CellROX analysis of hESC-derived cardiomyocytes exposed to increasing concentrations of XCT-790 (vehicle, n = 48; 1 μM, n = 48; 3 μM, n = 64; 10 μM, n = 39; n indicates technical replicates). (**D**) ERRα mRNA expression in hESC-derived cardiomyocytes exposed to increasing concentrations of XCT-790 (vehicle, n = 3; 1 μM, n = 6; 3 μM, n = 4; 10 μM, n = 4). (**E**) Peroxisome proliferator–activated receptor γ coactivator 1α (PGC-1α) mRNA expression in hESC-derived cardiomyocytes exposed to increasing concentrations of XCT-790 (vehicle, n = 4; 1 μM, n = 6; 3 μM, n = 6; 10 μM, n = 3). (**F**) CellROX analysis of adenoviral-infected H9C2 cells with control or hOPLAH adenoviral vector exposed to increasing concentration of XCT-790 (vehicle, n = 24; 1 μM, n = 24; 3 μM, n = 24; 10 μM, n = 16; n indicates technical replicates). (**G**) qRT-PCR mRNA expression of ERRα and OPLAH at different stages of development and IR injury [E12, n = 8; E18, n = 11; PP2, n = 7; 4 weeks, n = 3; 20 weeks (sham), n = 3; 20 weeks (IR), n = 3]. CellROX data are presented as fold change of RFU (A.U.) per microgram protein. Data are presented as means ± SEM. $^{*}P < 0.05$; $^{**}P < 0.01$; $^{***}P < 0.001$; $^{****}P < 0.0001$; $^{\#}P < 0.05$; $^{\#\#}P < 0.01$; $^{\#\#\#}P < 0.001$, as calculated by Student's t test or one-way ANOVA. "*" indicates significant difference compared to control, whereas "#" denotes differences between groups other than control. n indicates the number of biological replicates of cell experiments.

DISCUSSION

In response to stress, including hypoxia and hypertrophy, cardiac muscle suppresses postnatal gene expression and reactivates fetal genes. This process is mainly characterized by the metabolic switch in energy substrate from fatty acids (postnatal) to carbohydrates (fetal) (*2*). Using RNA-seq, we identified several known and previously unknown genes involved in this process, which were highly enriched for metabolic (*Hadh* and *MCCC1*) and cardiac disease pathways (*Cacna2d1* and *Ryr2*). One of the identified genes not previously associated with cardiac disease or development was *Oplah*. We demonstrated that OPLAH has cardioprotective properties and identified 5-oxoproline, the substrate of OPLAH, as a putative oxidative stress HF marker with diagnostic and prognostic potential in the clinical setting.

OPLAH is a gene that encodes for 5-oxoprolinase, an enzyme involved in the γ-glutamyl cycle (*5*, *6*). We identify *OPLAH* as a novel cardiac gene involved in HF, which is at least, in part, regulated by the PGC-1α/ERRα axis. Both PGC-1α and ERRα are key transcriptional regulators of antioxidant protection genes (*23*). It has been well established that PGC-1α regulates ERRα expression and that the expression of PGC-1α is induced in cardiac development and repressed in HF (*22*, *23*). Our data support the interaction between PGC-1α and ERRα by demonstrating that direct inhibition of ERRα activity results in an increase in PGC-1α and ERRα mRNA, suggesting a compensatory mechanism. Furthermore, the decreased activity of ERRα was shown to reduce OPLAH expression and enhance oxidative stress. These observations are in line with a recent study, which demonstrated by microarray analysis on RNA isolated from ERRα knockout mouse hearts that these mice had significantly increased the expression of PGC-1α and reduced OPLAH (*19*).

Here, the consequence of OPLAH depletion in HF is an increase in oxidative stress and 5-oxoproline. Furthermore, exogenous administration of 5-oxoproline to cardiomyocytes also led to increased oxidative stress. This finding is supported by a previous study that identified 5-oxoproline as an inducer of oxidative stress in brain tissue (*17*, *18*). We propose that HF leads to the reduction of PGC-1α, which, as a consequence, results in a decrease in ERRα and antioxidant protection genes, including OPLAH. Because of reduced OPLAH expression, 5-oxoproline cannot be processed into glutamate, and the excessive accumulation of 5-oxoproline leads to increases in oxidative stress, adding further insult to the progression of the disease (fig. S13). By exposing mice with cardiac-specific OPLAH overexpression to cardiac injury, we demonstrate that these mice have less oxidative stress,

lower 5-oxoproline, and reduced fibrosis, resulting in improved cardiac function. Thus, we posit that OPLAH is a potential target for therapeutic intervention in HF.

5-Oxoproline was elevated not only in the myocardium but also in the plasma of animals with HF. This suggests that accumulation of intracellular 5-oxoproline leads to diffusion or active transport of 5-oxoproline out of the cell, a notion supported by the identification of SLC5A8 and SLC16A1 as active transporters of 5-oxoproline in the kidney and brain cells, respectively (*29*, *30*). In HF, circulating 5-oxoproline was independently associated with patient outcome and associated with known markers for cardiac remodeling, stretch, and oxidative stress, but not with markers for inflammation. These findings, in line with our in vitro and in vivo work, suggest that 5-oxoproline is an oxidative stress marker with possible diagnostic and prognostic potential. However, it is still uncertain whether the increase in circulating 5-oxoproline in HF is a direct cause of reduced OPLAH in the cardiac tissue or whether 5-oxoproline is also secreted from other organs in response to HF. Besides the heart, OPLAH is also expressed in the kidneys, and hence, cardiac damage leading to renal failure may also result in increased 5-oxoproline production in the kidney. In our experimental setting, we observed that mice overexpressing OPLAH had reduced 5-oxoproline, resulting in an improved cardiac function after cardiac injury. The positive association of increased 5-oxoproline with adverse outcomes in HF patients supports the hypothesis of this study that OPLAH has a cardioprotective effect by reducing 5-oxoproline. However, further work in the human setting is needed to investigate whether reducing 5-oxoproline in patients with HF is beneficial. In addition, the clinical significance of 5-oxoproline as a prognostic biomarker has to be proven in future studies.

Our translational approach provides insights into the cardiac fetal-like gene program and its role in the failing heart. Here, we characterized

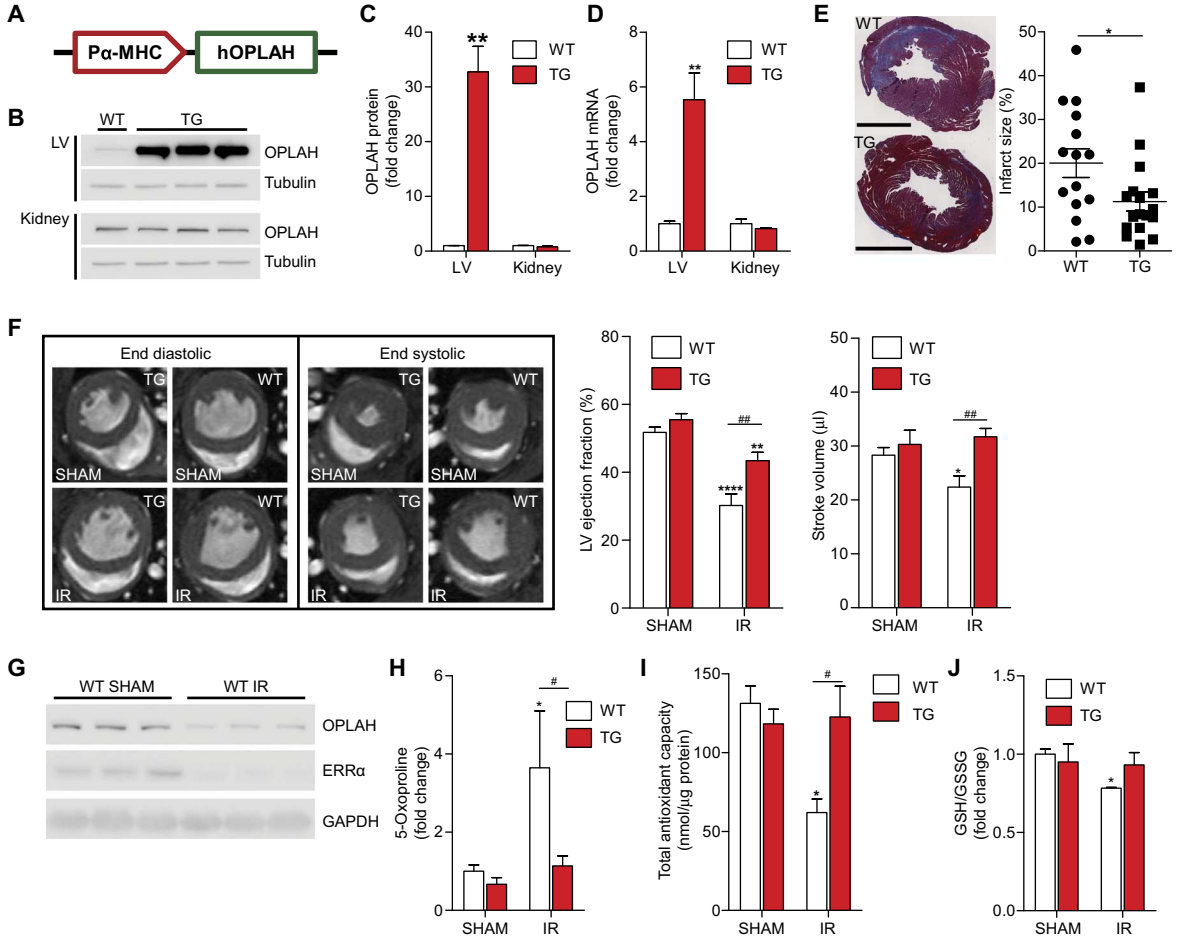

Fig. 4. OPLAH-TG mice have improved cardiac function after IR injury. (**A**) Construct used to develop the OPLAH-TG (TG) mice. (**B** to **D**) OPLAH expression in LV and kidney tissue of TG and WT mice (n = 12 and 4, respectively). (B) Representative immunoblotting analysis of OPLAH protein. (C) Quantified OPLAH protein. (D) Quantified OPLAH mRNA. (**E**) Representative LV tissue sections with Masson's trichrome staining of TG and WT after IR (scale bars, 2 mm) and quantification of infarct size (TG IR, n = 17; WT IR, n = 15). (**F**) Representative MRI images of WT and TG mouse hearts, and summary of LV ejection fraction and stroke volume (TG sham, n = 6; TG IR, n = 17; WT sham, n = 15; WT IR, n = 15). (**G**) Representative immunoblotting analysis of OPLAH and ERRα protein expression in the left ventricle of WT sham and IR mice. GAPDH, glyceraldehyde phosphate dehydrogenase. (**H**) 5-Oxoproline concentrations in LV tissue from TG versus WT mice 4 weeks after IR injury (TG sham, n = 9; TG IR, n = 8; WT sham, n = 11; WT IR, n = 7). (**I**) TAC of LV tissue from TG versus WT mice 4 weeks after IR injury (n = 3). (**J**) GSH/GSSG ratio present in LV tissue from TG versus WT mice 4 weeks after IR injury. Data are presented as fold change of microgram GSH/GSSG per microgram protein (TG sham, n = 3; TG IR, n = 4; WT sham, n = 4; WT IR n = 4). Data are presented as means ± SEM. $^{*}P < 0.05$; $^{**}P < 0.01$; $^{****}P < 0.0001$; $^{\#}P < 0.05$; $^{\#\#}P < 0.01$, as calculated by Student's t test or one-way ANOVA. "*" indicates significant difference compared to control, whereas "#" denotes differences between groups other than control. n indicates the number of animals.

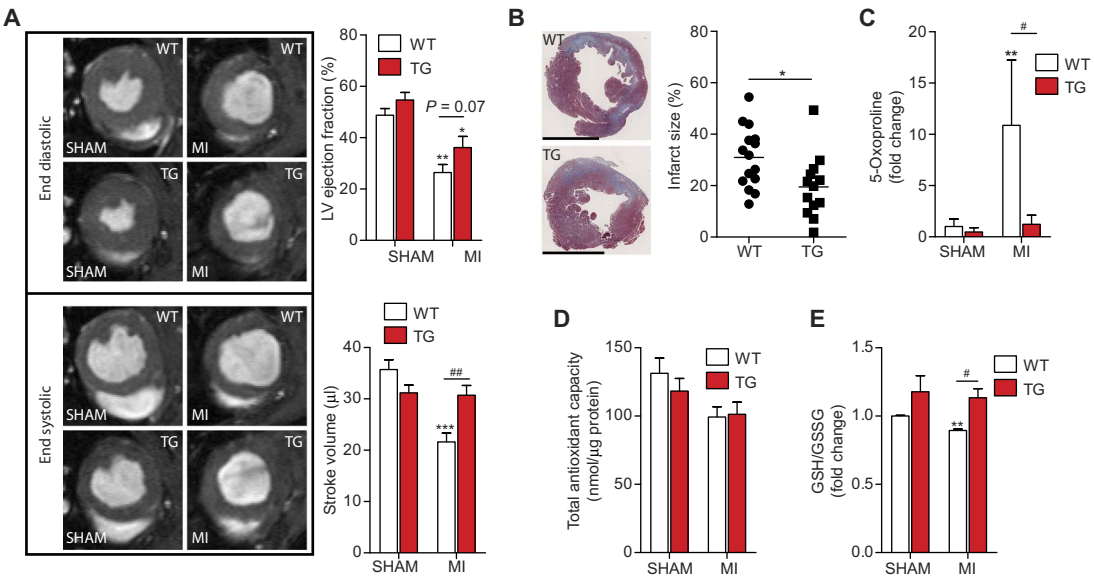

Fig. 5. OPLAH-TG mice show improved cardiac function after MI. (**A**) Representative MRI images of sham and MI hearts of WT and TG mice, and summary of LV ejection fraction and stroke volume (TG sham, $n = 6$; TG MI, $n = 13$; WT sham, $n = 6$; WT MI, $n = 15$). (**B**) Representative LV tissue sections with Masson's trichrome staining of TG and WT (scale bars, 3 mm), and summary infarct size (TG MI, $n = 13$; WT MI, $n = 15$). (**C**) 5-Oxoproline concentrations (in micromolars per microgram protein) in LV tissue from TG versus WT mice 4 weeks after MI (TG sham, $n = 5$; TG IR, $n = 6$; WT sham, $n = 5$; WT IR, $n = 6$). (**D**) TAC of LV tissue from TG versus WT mice 4 weeks after MI ($n = 3$). (**E**) GSH/GSSG ratio present in LV tissue from TG versus WT mice 4 weeks after MI. Data are presented as fold change of microgram GSH/GSSG per microgram protein ($n = 3$). Data are presented as means ± SEM. $^{*}P < 0.05$; $^{**}P < 0.01$; $^{***}P < 0.001$; $^{\#}P < 0.05$; $^{\#\#}P < 0.01$, as calculated by Student's t test or one-way ANOVA. "*" indicates significant difference compared to control, whereas "#" denotes differences between groups other than control. n indicates the number of animals.

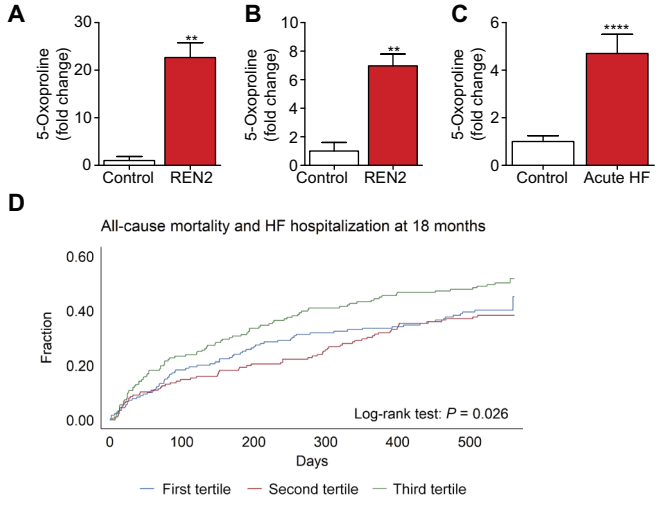

Fig. 6. Circulating 5-oxoproline in murine and human HF. (**A**) 5-Oxoproline concentration in LV tissue of REN2 rats ($n = 5$) compared to control Sprague Dawley rats ($n = 4$). (**B**) 5-Oxoproline concentrations in the plasma from control Sprague Dawley rats ($n = 4$) versus renin overexpression TG Sprague Dawley rats (REN2; $n = 5$). (**C**) 5-Oxoproline concentration in the human plasma from healthy controls (control; $n = 10$) and acute HF patients ($n = 10$). (**D**) Kaplan-Meier plot of all-cause mortality and HF hospitalization at 18 months in COACH HF patients. Patient population is divided into tertiles of plasma 5-oxoproline concentrations (T1, 3.2 to 9.2 µM; T2, 9.3 to 13.2 µM; T3, 13.3 to 35.0 µM). 5-Oxoproline concentrations (in micromolars per microgram protein) are presented as fold change. Data are presented as means ± SEM $^{**}P < 0.01$; $^{****}P < 0.0001$, as calculated by Student's t test. "*" indicates significant difference compared to control. n indicates the number of animals or individual human samples.

OPLAH, a novel cardiac gene with protective properties, and its substrate, 5-oxoproline, a putative circulating marker for predicting adverse outcome in patients with HF. Increased efforts in dissecting and modulating the cardiac fetal-like gene program may result in better understanding of genes involved in HF, leading to potential novel diagnostic, prognostic, and therapeutic options in these patients.

MATERIALS AND METHODS

Study design

The main research objective was to identify genes associated with the fetal gene program, leading to the identification of *OPLAH* as a relevant gene in cardiac development and HF. We used rodent disease models, genetically modified mice, and human plasma samples to study its importance in cardiac disease and protection supported by in vitro mechanistic data. The mice were assigned randomly to the experimental groups and were analyzed in a blinded fashion. The number of animals, experimental replicates, and patient samples is described in the figure legends.

Next-generation sequencing tissue acquisition and RNA extraction

All animal protocols were approved by the Animal Ethical Committee of the University of Groningen (permit number DEC6002AA). A total of four stages of murine cardiac development (E12, E18, PP2, and 4 weeks) were used in this study. Female mice at days 12 and 18 of pregnancy were sacrificed, followed by the excision of the embryos. For E12, the whole heart was removed for each embryo. At E18, the left ventricle was excised from the embryos. The left ventricle of PP2 pups were removed after decapitation. Four-week-old mice were sacrificed after which the left ventricle was isolated. We also included 20-week-old mice that had undergone IR injury or sham treatment. For each time point, we used $n = 3$ samples, and all tissue samples were snap-frozen after excision and stored at −80°C until total RNA was isolated by the TRIzol RNA isolation protocol.

RNA-seq library preparation and sequencing

RNA-seq was performed on the same 18 mice samples that were used for the qRT-PCR analysis. The quality of extracted RNA was accessed

on a Bioanalyzer 2100 (Agilent) using a Pico RNA chip (Agilent). All samples passed quality control, exceeding a minimum RNA integrity number of 8. Then, 1 μg of total RNA from each sample was processed with the NEXTflex Poly(A) Beads kit (Bioo Life Science) to pull down the mRNA from the total RNA samples. Eluted mRNA was further used for library preparation. Libraries were generated by strictly following NEXTflex Illumina RNA-Seq Library Prep version 2 kit recommendations (Bioo Life Science). At the end of the procedure, libraries were purified with AMPure XP beads, and the DNA was eluted with 30 μl of resuspension buffer. The size and quality of the libraries were controlled by running them on a Bioanalyzer 2100 using the High Sensitivity DNA assay. For sequencing, all 18 samples were pooled together. This 2 nM pool was made equimolar with individual library concentrations calculated from Qubit dsDNA HS Assay kit data and library peak size derived from Bioanalyzer data. The libraries were sequenced on the Illumina HiSeq 2500 machine in the RapidRun mode.

Analysis of RNA-seq data

Reads were mapped to the mouse genome assembly GRCm38 using STAR aligner version 2.5.2b (*31*). Gene counts were derived from the alignment files using the htseq-count program version 0.6.1p1 from HTSeq package (*32*) and Ensembl gene annotations. Differential gene expression between pairs of conditions was calculated using edgeR package (*33*) with batch effects correction and upper quartile normalization. Genes with FDR of ≤0.05 were considered as statistically significant. For linear regression analysis of gene expression during development, a custom script based on Perl::PDL library (http://pdl.perl.org) was used. Genes with P values of ≤0.05 after Bonferroni correction were considered as statistically significant.

Cell culture

For a detailed description of cell lines and culturing protocols, see Supplementary Materials and Methods.

Viral constructs

To generate recombinant adenoviral vectors, the ViraPower Adenoviral Expression System (Invitrogen) was used according to the manufacturer's instructions. OPLAH-specific shRNA–targeting oligonucleotides (table S14) were cloned into a pENTR4 vector containing an H1 promoter and a green fluorescent protein marker gene. For the OPLAH overexpression construct, the full-length human OPLAH complementary DNA (cDNA) was N-terminally fused with a myc tag and cloned into the pENTR4 vector. Recombinant adenovirus was generated as previously described (*34*). All constructs were verified by sequencing, and NRVCs were infected with an adenoviral multiplicity of infection of 50.

In vitro oxidative stress

In vitro oxidative stress was achieved by culturing cells under hypoxic conditions or by the addition of H_2O_2. Additional information is provided in Supplementary Materials and Methods.

CellROX

Oxidative stress was measured by means of CellROX Orange Reagent (Thermo Fisher Scientific), as per the manufacturer's instructions. For additional information, see Supplementary Materials and Methods.

Total antioxidant capacity

The antioxidant capacity of tissue samples was measured by means of the Total Antioxidant Capacity Assay kit (ab65329, Abcam), as per the manufacturer's instructions. For additional information, see Supplementary Materials and Methods.

GSH/GSSG measurements

GSH and GSSG were measured by means of the Glutathione Fluorometric Assay kit (#K26-100, BioVision), as per the manufacturer's instructions. See Supplementary Materials and Methods for details.

Quantitative real-time PCR

Details of qRT-PCR are provided in Supplementary Materials and Methods. Primer sequences can be found in table S15.

Western blotting

Details regarding Western blotting are provided in Supplementary Materials and Methods. Antibodies used are described in table S16.

TG renin overexpression rats

Animal protocol was approved by the Animal Ethical Committee of the University of Groningen (permit number DEC5163). The male homozygous TGR (mREN2)27 rats (denoted as REN2) were bred and obtained from the Max Delbrück Center for Molecular Medicine. These rats have an overexpression of the mouse renin and develop severe hypertension and LV hypertrophy, leading to HF at 13 to 15 weeks of age (*35*). We used five 12- to 14-week-old male REN2 rats and four male age-matched Sprague Dawley rats as control (Harlan). Before scarification, an echocardiogram and hemodynamic measurements were performed. Animals were housed under standard conditions.

OPLAH-TG mice

The animal protocol was approved by the Animal Ethical Committee of the University of Groningen (permit number DEC6632A). The animal experiments that were performed conform with the ARRIVE (Animal Research: Reporting of In Vivo Experiments) guidelines. The human OPLAH gene (GenBank no. NM_017570.4) was amplified by PCR using primers containing Sal I and Hind III restriction sites (table S14). The PCR product was cloned into a previously described vector containing the cardiac-specific myosin heavy chain (α-MHC) promoter (*36*). The BamH I fragment of this construct, containing the α-MHC promoter and human OPLAH cDNA sequence, was subsequently used for pronuclear injection to generate cardiac-specific human OPLAH-TG mice (FVB background). These TG mice were made by the mouse clinic for aging research (University Medical Center Groningen) in collaboration with Mayo Clinic. The mice were backcrossed with C57BL/6 mice, and third-generation backcrossed animals (N3) were used in this study. In all experiments performed in this study, age- and sex-matched non-TG (WT) littermates were used for comparison with the OPLAH-TG mice.

Rodent models of HF

All animal protocols were approved by the Animal Ethical Committee of the University of Groningen. The animal experiments that were performed conform with the ARRIVE guidelines. Animals were housed under standard conditions. For animal experiments involving TG animals, the surgeon tried to achieve a ±30% area at risk of the left ventricle and was blinded to which animal was WT and which was TG. Details regarding the implementation of rat MI, murine MI, and murine IR models are described in Supplementary Materials and Methods.

Echocardiography and cardiac MRI measurements

Cardiac function of rats was assessed by means of echocardiography at baseline and before scarification with a Vivid 7 (GE Healthcare) equipped with a 10-MHz phase array linear transducer, as previously described (*36*). Cardiac MRI was performed as previously described (*37*). For additional information, see Supplementary Materials and Methods.

Hemodynamic measurements

Heart rate and pressures of the aorta and left ventricle were measured after 4 weeks using the Scisense ADVantage pressure-volume (PV) measurement system with a PV catheter, as previously described (*38*). For additional information, see Supplementary Materials and Methods.

Histology

For immunohistochemical analysis, hearts were fixed overnight with 10% neutral-buffered formalin at 4°C. After fixation, samples were subjected to a dehydration series, embedded in paraffin, and cut into 4 μM sections. Masson's trichrome, fluorescein isothiocyanate–labeled wheat germ agglutinin (WGA), and cleaved Caspase-3 stainings were performed. Quantification was performed with the Aperio ImageScope software (Masson's trichrome) and Fiji for the WGA and cleaved Caspase-3 stainings (*39*). The investigators were blinded to experimental settings during data analysis. For additional information, see Supplementary Materials and Methods.

Human patient population and plasma samples

A subpopulation of the Coordinating Study Evaluating Outcomes of Advising and Counseling in Heart Failure (COACH) was used. Briefly, 1023 patients were included to participate in a prospective randomized disease management study. The rationale and outcomes of this trail have been reported elsewhere (*26*–*28*). Samples for biomarker analysis were obtained from a subset of 567 patients, who were representative of the entire study population on baseline characteristics. Blood sampling was performed before discharge, when patients were stabilized after an acute HF admission, and samples were immediately stored at −80°C until the analysis was performed. This study complies with the Declaration of Helsinki, and local medical ethics committees approved the study. All patients provided written informed consent.

Here, 535 patient plasma samples from the 567 previously described samples were analyzed. Of the remaining 32 patients, no plasma was available for 5-oxoproline measurements, and these patients were excluded from this analysis. The subpopulation of 535 patients remained representative for the entire study population on baseline characteristics (table S9). The primary end point of the COACH study was the combined end point of all-cause mortality or rehospitalization at 18 months, where rehospitalization was defined as an unplanned overnight hospital stay connected to worsening HF. All events were evaluated and adjudicated by an independent end point committee. Blood sampling was performed before discharge, and samples were immediately stored at −80°C until the analysis was performed. Measurements of the available biomarkers have been previously described (*25*).

Internal standard preparation (^{13}C-5-oxoproline and L-glutamic acid) and validation of the analytical method

5-Oxoproline internal standard (IS) was prepared from ^{13}C-labeled L-glutamic acid (*40*). Following international guidelines (*41*, *42*), method validation was performed by evaluating the following parameters: intraday variability (repeatability), interday variability (intermediate precision), lower limit of quantification, linearity, and accuracy (fig. S14 and tables S17 and S18). For additional information, see Supplementary Materials and Methods.

Sample preparation procedure

For plasma sample preparation, 5 μl of animal plasma or 25 μl of human plasma was mixed with 200 μl of the extraction solution (25 μl of 5-oxoproline IS in 75% methanol). For murine LV tissue sample preparation, about 1 mg of powdered tissue was homogenized in 200 μl of extraction solution. Samples were vortex-mixed and centrifuged for 10 min at 20,000*g*. Supernatant was dried under a stream of nitrogen gas at room temperature, followed by resuspension in 100 μl of water. At this stage, samples were stored at −80°C until LC-MS measurements were performed. For tissue samples, 5-oxoproline and L-glutamic acid concentrations were corrected for the amount of total protein (per microgram).

LC-MS of 5-oxoproline and L-glutamic acid

5-Oxoproline and L-glutamic acid were separated in the HILIC (hydrophilic interaction liquid chromatography) mode using a Luna NH_2 column (3 μm; 100 × 2 mm; Phenomenex) on an Agilent 1290 Infinity LC system. Mass spectrometry detection was performed using an Agilent 6410 triple quadrupole system. For additional information, see Supplementary Materials and Methods.

Statistical analysis

All animal and cell experimental data are represented as means ± SEM. To compare the difference between two groups, Student's *t* test was performed. Comparisons between more than two groups were carried out using one-way ANOVA with post hoc Bonferroni test. *P* values of <0.05 were considered statistically significant. All analyses were carried out using the GraphPad Prism software version 5.04 (GraphPad Software Inc.). For the animal experiments, we chose the sample sizes for all the groups based on the feasibility and prior knowledge of statistical power from previously published experiments (*35*–*37*, *43*, *44*). Parametric tests were chosen only when variances between the compared groups were not significantly different. With small sample sizes, we did not apply statistical tests for normality or equality of variances.

All human plasma data are represented as means ± SD or medians with interquartile ranges where appropriate. Comparisons between two or more groups were performed using one-way ANOVA or the Kruskal-Wallis test or χ^2 test where appropriate. For further analyses, concentrations of 5-oxoproline were $\log_2$-transformed to acquire a normal distribution. To investigate the relationship of 5-oxoproline with other biochemical markers, a linear regression was performed. A Kaplan-Meier graph shows the relationship of tertiles of 5-oxorpoline with the primary end point of all-cause mortality and HF-related rehospitalizations at 18 months. For multivariable outcome analyses, the relationship of tertiles of 5-oxoproline with outcome was studied using Cox regression analysis. The risk nadir was used as the reference group. Analyses were corrected for clinically relevant variables. $P < 0.05$ was considered statistically significant. All analyses were carried out using the Stata version 13.0 for Windows. For experiments where the total *n* was smaller than 20, individual subject level data are shown in table S19.

SUPPLEMENTARY MATERIALS

www.sciencetranslationalmedicine.org/cgi/content/full/9/415/eaam8574/DC1

Materials and Methods

Fig. S1. Top 29 novel cardiac fetal genes mRNA expression profiles across a human organ panel.

Fig. S2. OPLAH is localized in the cytosol of cardiomyocytes.
Fig. S3. OPLAH protein expression in HF animal models.
Fig. S4. Mechanical stretch results in oxidative stress and OPLAH depletion in NRVCs.
Fig. S5. Hypoxia induces oxidative stress and OPLAH depletion in NRVCs.
Fig. S6. H_2O_2 induces oxidative stress and OPLAH depletion in NRVCs.
Fig. S7. OPLAH short hairpin and overexpression constructs in NRVCs.
Fig. S8. ERRα is involved in the regulation of OPLAH in NRVCs.
Fig. S9. ERRα expression in NRVCs exposed to stretch, hypoxia, or H_2O_2.
Fig. S10. OPLAH-TG mice have reduced fibrosis compared to WT mice after IR injury.
Fig. S11. OPLAH-TG mice show no difference in LV hypertrophy compared to WT mice after IR injury or after MI.
Fig. S12. OPLAH-TG mice have reduced cleaved Caspase-3–positive cells in the left ventricle after MI.
Fig. S13. Schematic of OPLAH regulation in the cardiomyocyte.
Fig. S14. Calibration curves for LC-MS ISs ^{13}C-5-oxoproline and L-glutamic acid.
Table S1. Significantly up-regulated genes during murine cardiac development (provided as an Excel file).
Table S2. Significantly down-regulated genes during murine cardiac development (provided as an Excel file).
Table S3. Top cardiac fetal reprogramming genes (provided as an Excel file).
Table S4. Characteristics of renin overexpression rats (REN2) and Sprague Dawley rats.
Table S5. Characteristics of WT mice after IR injury.
Table S6. Characteristics of Sprague Dawley rats after MI.
Table S7. Characteristics of OPLAH overexpression (TG) and WT mice at baseline (sham) and after IR injury.
Table S8. Characteristics of OPLAH overexpression (TG) and WT mice at baseline (sham) and after MI.
Table S9. Baseline characteristics of all 535 patients compared to total COACH cohort (n = 1023).
Table S10. Baseline characteristics of all 535 patients at discharge, divided into tertiles of 5-oxoproline (in micromolars).
Table S11. Regression analyses of 5-oxoproline association with HF biomarkers.
Table S12. Regression analyses of multivariable model corrected for univariable associations.
Table S13. Survival analyses.
Table S14. OPLAH-specific shRNA–targeting oligonucleotides and cloning primers for human OPLAH overexpression.
Table S15. List of primers used in this study.
Table S16. List of antibodies used in this study.
Table S17. Accuracy and precision results for 5-oxoproline.
Table S18. Accuracy and precision results for L-glutamic acid.
Table S19. Individual subject level data for experiments with n < 20 (provided as an Excel file).

REFERENCES AND NOTES

1. P. Ponikowski, A. A. Voors, S. D. Anker, H. Bueno, J. G. F. Cleland, A. J. S. Coats, V. Falk, J. R. González-Juanatey, V.-P. Harjola, E. A. Jankowska, M. Jessup, C. Linde, P. Nihoyannopoulos, J. T. Parissis, B. Pieske, J. P. Riley, G. M. C. Rosano, L. M. Ruilope, F. Ruschitzka, F. H. Rutten, P. van der Meer; Authors/Task Force Members; Document Reviewers, 2016 ESC Guidelines for the diagnosis and treatment of acute and chronic heart failure. *Eur. J. Heart Fail.* **18**, 891–975 (2016).
2. H. Taegtmeyer, S. Sen, D. Vela, Return to the fetal gene program: A suggested metabolic link to gene expression in the heart. *Ann. N. Y. Acad. Sci.* **1188**, 191–198 (2010).
3. P. Razeghi, M. E. Young, J. L. Alcorn, C. S. Moravec, O. H. Frazier, H. Taegtmeyer, Metabolic gene expression in fetal and failing human heart. *Circulation* **104**, 2923–2931 (2001).
4. Z. Yin, J. Ren, W. Guo, Sarcomeric protein isoform transitions in cardiac muscle: A journey to heart failure. *Biochim. Biophys. Acta* **1852**, 47–52 (2015).
5. A. Meister, M. E. Anderson, Glutathione. *Annu. Rev. Biochem.* **52**, 711–760 (1983).
6. Y. Liu, A. S. Hyde, M. A. Simpson, J. J. Barycki, Emerging regulatory paradigms in glutathione metabolism. *Adv. Cancer Res.* **122**, 69–101 (2014).
7. V. Şapira, I. M. Cojocaru, G. Socoliuc, G. Lilios, M. Grigorian, E. Craiu, M. Cojocaru, Glutathione reductase levels in patients with unstable angina. *Rom. J. Intern. Med.* **49**, 197–201 (2011).
8. E. Ruttmann, L. J. Brant, H. Concin, G. Diem, K. Rapp, H. Ulmer; Vorarlberg Health Monitoring and Promotion Program Study Group, γ-Glutamyltransferase as a risk factor for cardiovascular disease mortality: An epidemiological investigation in a cohort of 163,944 Austrian adults. *Circulation* **112**, 2130–2137 (2005).
9. C. Adamy, P. Mulder, L. Khouzami, N. Andrieu-abadie, N. Defer, G. Candiani, C. Pavoine, P. Caramelle, R. Souktani, P. Le Corvoisier, M. Perier, M. Kirsch, T. Damy, A. Berdeaux, T. Levade, C. Thuillez, L. Hittinger, F. Pecker, Neutral sphingomyelinase inhibition participates to the benefits of *N*-acetylcysteine treatment in post-myocardial infarction failing heart rats. *J. Mol. Cell. Cardiol.* **43**, 344–353 (2007).
10. T. Damy, M. Kirsch, L. Khouzami, P. Caramelle, P. Le Corvoisier, F. Roudot-Thoraval, J.-L. Dubois-Randé, L. Hittinger, C. Pavoine, F. Pecker, Glutathione deficiency in cardiac patients is related to the functional status and structural cardiac abnormalities. *PLOS ONE* **4**, e4871 (2009).
11. Y. Watanabe, K. Watanabe, T. Kobayashi, Y. Saito, D. Fujioka, T. Nakamura, J.-e Obata, K. Kawabata, H. Mishina, K. Kugiyama, Chronic depletion of glutathione exacerbates ventricular remodelling and dysfunction in the pressure-overloaded heart. *Cardiovasc. Res.* **97**, 282–292 (2013).
12. M. A. Forgione, A. Cap, R. Liao, N. I. Moldovan, R. T. Eberhardt, C. C. Lim, J. Jones, P. J. Goldschmidt-Clermont, J. Loscalzo, Heterozygous cellular glutathione peroxidase deficiency in the mouse: Abnormalities in vascular and cardiac function and structure. *Circulation* **106**, 1154–1158 (2002).
13. Y. Taur, W. H. Frishman, The cardiac ryanodine receptor (RyR2) and its role in heart disease. *Cardiol. Rev.* **13**, 142–146 (2005).
14. C. Antzelevitch, G. D. Pollevick, J. M. Cordeiro, O. Casis, M. C. Sanguinetti, Y. Aizawa, A. Guerchicoff, R. Pfeiffer, A. Oliva, B. Wollnik, P. Gelber, E. P. Bonaros, E. Burashnikov, Y. Wu, J. D. Sargent, S. Schickel, R. Oberheiden, A. Bhatia, L.-F. Hsu, M. Haïssaguerre, R. Schimpf, M. Borggrefe, C. Wolpert, Loss-of-function mutations in the cardiac calcium channel underlie a new clinical entity characterized by ST-segment elevation, short QT intervals, and sudden cardiac death. *Circulation* **115**, 442–449 (2007).
15. A. El-Armouche, N. Ouchi, K. Tanaka, G. Doros, K. Wittköpper, T. Schulze, T. Eschenhagen, K. Walsh, F. Sam, Follistatin-like 1 in chronic systolic heart failure: A marker of left ventricular remodeling. *Circ. Heart Fail.* **4**, 621–627 (2011).
16. A. V. Villar, R. García, M. Llano, M. Cobo, D. Merino, A. Lantero, M. Tramullas, J. M. Hurlé, M. A. Hurlé, J. F. Nistal, BAMBI (BMP and activin membrane-bound inhibitor) protects the murine heart from pressure-overload biomechanical stress by restraining TGF-β signaling. *Biochim. Biophys. Acta* **1832**, 323–335 (2013).
17. C. D. Pederzolli, Â. M. Sgaravatti, C. A. Braum, C. C. Prestes, G. K. Zorzi, M. B. Sgarbi, A. T. S. Wyse, C. M. D. Wannmacher, M. Wajner, C. S. Dutra-Filho, 5-Oxoproline reduces non-enzymatic antioxidant defenses in vitro in rat brain. *Metab. Brain Dis.* **22**, 51–65 (2007).
18. C. D. Pederzolli, C. P. Mescka, B. R. Zandoná, D. de Moura Coelho, Â. M. Sgaravatti, M. B. Sgarbi, A. T. de Souza Wyse, C. M. Duval Wannmacher, M. Wajner, C. R. Vargas, C. S. Dutra-Filho, Acute administration of 5-oxoproline induces oxidative damage to lipids and proteins and impairs antioxidant defenses in cerebral cortex and cerebellum of young rats. *Metab. Brain Dis.* **25**, 145–154 (2010).
19. C. R. Dufour, B. J. Wilson, J. M. Huss, D. P. Kelly, W. A. Alaynick, M. Downes, R. M. Evans, M. Blanchette, V. Giguère, Genome-wide orchestration of cardiac functions by the orphan nuclear receptors ERRα and γ. *Cell Metab.* **5**, 345–356 (2007).
20. K. F. Cunningham, G. C. Beeson, C. C. Beeson, C. F. Baicu, M. R. Zile, P. J. McDermott, Estrogen-Related Receptor α (ERRα) is required for adaptive increases in PGC-1 isoform expression during electrically stimulated contraction of adult cardiomyocytes in sustained hypoxic conditions. *Int. J. Cardiol.* **187**, 393–400 (2015).
21. P. Coward, D. Lee, M. V. Hull, J. M. Lehmann, 4-Hydroxytamoxifen binds to and deactivates the estrogen-related receptor γ. *Proc. Natl. Acad. Sci. U.S.A.* **98**, 8880–8884 (2001).
22. G. C. Rowe, A. Jiang, Z. Arany, PGC-1 coactivators in cardiac development and disease. *Circ. Res.* **107**, 825–838 (2010).
23. J. M. Huss, I. P. Torra, B. Staels, V. Giguère, D. P. Kelly, Estrogen-related receptor α directs peroxisome proliferator-activated receptor α signaling in the transcriptional control of energy metabolism in cardiac and skeletal muscle. *Mol. Cell. Biol.* **24**, 9079–9091 (2004).
24. B. G. Demissei, M. A. E. Valente, J. G. Cleland, C. M. O'Connor, M. Metra, P. Ponikowski, J. R. Teerlink, G. Cotter, B. Davison, M. M. Givertz, D. M. Bloomfield, H. Dittrich, P. van der Meer, D. J. van Veldhuisen, H. L. Hillege, A. A. Voors, Optimizing clinical use of biomarkers in high-risk acute heart failure patients. *Eur. J. Heart Fail.* **18**, 269–280 (2016).
25. J. Tromp, A. van der Pol, I. T. Klip, R. A. de Boer, T. Jaarsma, W. H. van Gilst, A. A. Voors, D. J. van Veldhuisen, P. van der Meer, Fibrosis marker syndecan-1 and outcome in patients with heart failure with reduced and preserved ejection fraction. *Circ. Heart Fail.* **7**, 457–462 (2014).
26. T. Jaarsma, M. H. L. van der Wal, J. Hogenhuis, I. Lesman, M.-L. A. Luttik, N. J. G. M. Veeger, D. J. van Veldhuisen, Design and methodology of the COACH study: A multicenter randomised Coordinating study evaluating Outcomes of Advising and Counselling in Heart failure. *Eur. J. Heart Fail.* **6**, 227–233 (2004).
27. T. Jaarsma, M. H. L. van der Wal, I. Lesman-Leegte, M.-L. Luttik, J. Hogenhuis, N. J. Veeger, R. Sanderman, A. W. Hoes, W. H. van Gilst, D. J. A. Lok, P. H. J. M. Dunselman, J. G. P. Tijssen, H. L. Hillege, D. J. van Veldhuisen; Coordinating Study Evaluating Outcomes of Advising and Counseling in Heart Failure (COACH) Investigators, Effect of moderate or intensive disease management program on outcome in patients with heart failure: Coordinating Study Evaluating Outcomes of Advising and Counseling in Heart Failure (COACH). *Arch. Intern. Med.* **168**, 316–324 (2008).
28. D. J. van Veldhuisen, G. C. M. Linssen, T. Jaarsma, W. H. van Gilst, A. W. Hoes, J. G. P. Tijssen, W. J. Paulus, A. A. Voors, H. L. Hillege, B-type natriuretic peptide and prognosis in heart

failure patients with preserved and reduced ejection fraction. *J. Am. Coll. Cardiol.* **61**, 1498–1506 (2013).
29. S. Sasaki, Y. Futagi, M. Kobayashi, J. Ogura, K. Iseki, Functional characterization of 5-oxoproline transport via SLC16A1/MCT1. *J. Biol. Chem.* **290**, 2303–2311 (2015).
30. S. Miyauchi, E. Gopal, E. Babu, S. R. Srinivas, Y. Kubo, N. S. Umapathy, S. V. Thakkar, V. Ganapathy, P. D. Prasad, Sodium-coupled electrogenic transport of pyroglutamate (5-oxoproline) via SLC5A8, a monocarboxylate transporter. *Biochim. Biophys. Acta* **1798**, 1164–1171 (2010).
31. A. Dobin, C. A. Davis, F. Schlesinger, J. Drenkow, C. Zaleski, S. Jha, P. Batut, M. Chaisson, T. R. Gingeras, STAR: Ultrafast universal RNA-seq aligner. *Bioinformatics* **29**, 15–21 (2013).
32. S. Anders, P. T. Pyl, W. Huber, HTSeq—A Python framework to work with high-throughput sequencing data. *Bioinformatics* **31**, 166–169 (2015).
33. M. D. Robinson, D. J. McCarthy, G. K. Smyth, edgeR: A Bioconductor package for differential expression analysis of digital gene expression data. *Bioinformatics* **26**, 139–140 (2010).
34. B. Lu, W. Tigchelaar, W. P. T. Ruifrok, W. H. van Gilst, R. A. de Boer, H. H. W. Silljé, *DHRS7c*, a novel cardiomyocyte-expressed gene that is down-regulated by adrenergic stimulation and in heart failure. *Eur. J. Heart Fail.* **14**, 5–13 (2012).
35. W.-P. T. Ruifrok, C. Qian, H. H. W. Silljé, H. van Goor, D. J. van Veldhuisen, W. H. van Gilst, R. A. de Boer, Heart failure-associated anemia: Bone marrow dysfunction and response to erythropoietin. *J. Mol. Med.* **89**, 377–387 (2011).
36. M. V. Cannon, H. H. W. Silljé, J. W. A. Sijbesma, I. Vreeswijk-Baudoin, J. Ciapaite, B. van der Sluis, J. van Deursen, G. J. J. Silva, L. J. de Windt, J.-Å. Gustafsson, P. van der Harst, W. H. van Gilst, R. A. de Boer, Cardiac LXRα protects against pathological cardiac hypertrophy and dysfunction by enhancing glucose uptake and utilization. *EMBO Mol. Med.* **7**, 1229–1243 (2015).
37. H. G. Booij, H. Yu, R. A. De Boer, C. W. A. van de Kolk, B. van de Sluis, J. M. Van Deursen, W. H. Van Gilst, H. H. W. Silljé, B. D. Westenbrink, Overexpression of A kinase interacting protein 1 attenuates myocardial ischaemia/reperfusion injury but does not influence heart failure development. *Cardiovasc. Res.* **111**, 217–226 (2016).
38. L. M. G. Meems, M. V. Cannon, H. Mahmud, A. A. Voors, W. H. van Gilst, H. H. W. Silljé, W. P. T. Ruifrok, R. A. de Boer, The vitamin D receptor activator paricalcitol prevents fibrosis and diastolic dysfunction in a murine model of pressure overload. *J. Steroid Biochem. Mol. Biol.* **132**, 282–289 (2012).
39. J. Schindelin, I. Arganda-Carreras, E. Frise, V. Kaynig, M. Longair, T. Pietzsch, S. Preibisch, C. Rueden, S. Saalfeld, B. Schmid, J.-Y. Tinevez, D. J. White, V. Hartenstein, K. Eliceiri, P. Tomancak, A. Cardona, Fiji: An open-source platform for biological-image analysis. *Nat. Methods* **9**, 676–682 (2012).
40. J. A. Eckstein, G. M. Ammerman, J. M. Reveles, B. L. Ackermann, Analysis of glutamine, glutamate, pyroglutamate, and GABA in cerebrospinal fluid using ion pairing HPLC with positive electrospray LC/MS/MS. *J. Neurosci. Methods* **171**, 190–196 (2008).
41. Committee for Medicinal Products for Human Use, "Guideline on bioanalytical method validation" (European Medicines Agency, 2012); www.ema.europa.eu/docs/en_GB/document_library/Scientific_guideline/2011/08/WC500109686.pdf.
42. U.S. Department of Health and Human Services, Food and Drug Administration, Center for Drug Evaluation and Research, Center for Veterinary Medicine, "Guidance for industry: Bioanalytical method validation" (Food and Drug Administration, 2001); www.fda.gov/downloads/Drugs/Guidance/ucm070107.pdf.
43. P. M. Snijder, R. A. de Boer, E. M. Bos, J. C. van den Born, W.-P. T. Ruifrok, I. Vreeswijk-Baudoin, M. C. R. F. van Dijk, J.-L. Hillebrands, H. G. D. Leuvenink, H. van Goor, Gaseous hydrogen sulfide protects against myocardial ischemia-reperfusion injury in mice partially independent from hypometabolism. *PLOS ONE* **8**, e63291 (2013).
44. M. H. T. Hartman, I. Vreeswijk-Baudoin, H. E. Groot, K. W. A. van de Kolk, R. A. de Boer, I. Mateo Leach, R. Vliegenthart, H. H. W. Sillje, P. van der Harst, Inhibition of interleukin-6 receptor in a murine model of myocardial ischemia-reperfusion. *PLOS ONE* **11**, e0167195 (2016).

Acknowledgments: We thank M. Dokter, L. van Genne, and K. van de Kolk for their excellent technical assistance. **Funding:** This work was supported by the Innovational Research Incentives Scheme program of the Netherlands Organisation for Scientific Research (NWO; Veni grant 91610013) to P.v.d.M. **Author contributions:** A.v.d.P. and P.v.d.M. conceptualized and designed the study. A.v.d.P., A.G., H.H.W.S., E.S.O., I.V.-B., B.v.d.S., J.M.v.D., A.A.V., D.J.v.V., E.B., R.A.d.B., and R.B. acquired the data. A.v.d.P., A.G., J.T., I.V.-B., M.H., E.B., R.B., and P.v.d.M. analyzed and interpreted the data. A.G., H.H.W.S., B.v.d.S., J.M.v.D., A.A.V., D.J.v.V., R.A.d.B., and R.B. contributed reagents/materials/analysis tools. A.v.d.P. and P.v.d.M. drafted the manuscript. All authors critically reviewed the manuscript and approved the final of version for publication. **Competing interests:** The authors declare that they have no competing financial interests. **Data and materials availability:** RNA-seq data that support the findings in this study are available in the ArrayExpress database under accession number E-MTAB-5449.

Submitted 27 January 2017
Resubmitted 1 August 2017
Accepted 3 October 2017
Published 8 November 2017
10.1126/scitranslmed.aam8574

Citation: A. van der Pol, A. Gil, H. H. W. Silljé, J. Tromp, E. S. Ovchinnikova, I. Vreeswijk-Baudoin, M. Hoes, I. J. Domian, B. van de Sluis, J. M. van Deursen, A. A. Voors, D. J. van Veldhuisen, W. H. van Gilst, E. Berezikov, P. van der Harst, R. A. de Boer, R. Bischoff, P. van der Meer, Accumulation of 5-oxoproline in myocardial dysfunction and the protective effects of OPLAH. *Sci. Transl. Med.* **9**, eaam8574 (2017).

Science Translational Medicine

Accumulation of 5-oxoproline in myocardial dysfunction and the protective effects of OPLAH

Atze van der Pol, Andres Gil, Herman H. W. Silljé, Jasper Tromp, Ekaterina S. Ovchinnikova, Inge Vreeswijk-Baudoin, Martijn Hoes, Ibrahim J. Domian, Bart van de Sluis, Jan M. van Deursen, Adriaan A. Voors, Dirk J. van Veldhuisen, Wiek H. van Gilst, Eugene Berezikov, Pim van der Harst, Rudolf A. de Boer, Rainer Bischoff and Peter van der Meer

Sci Transl Med **9**, eaam8574.
DOI: 10.1126/scitranslmed.aam8574

A fetal gene for heart failure

One way the heart responds to cardiac injury is by reverting gene expression to developmental patterns. Van der Pol *et al*. discovered that *Oplah*, a gene encoding an enzyme that converts 5-oxoproline to glutamate as part of the γ-glutamyl cycle, was repressed in adult mouse hearts with heart failure. Depleting *Oplah* in cardiomyocytes increased 5-oxoproline and oxidative stress, and elevated 5-oxoproline in blood samples from patients with heart failure was associated with worse outcome. Overexpressing *OPLAH* protected mice from cardiac injury in models of heart failure, suggesting that *OPLAH* and other fetal-like genes could be therapeutic targets.